



---

*Research article*

## **A new APSO-SPC method for parameter identification problem with uncertainty caused by random measurement errors**

**Peng Zhong, Xuanlong Wu\*, Li Zhu and Aohao Yang**

State Key Laboratory of Structural Analysis, Optimization and CAE Software for Industrial Equipment, School of Mechanics and Aerospace Engineering, Dalian University of Technology, Dalian 116024, China

\* **Correspondence:** Email: [wuxuanlong7895@mail.dlut.edu.cn](mailto:wuxuanlong7895@mail.dlut.edu.cn).

**Abstract:** In parameter identification problem, errors are common in measurement data, resulting in uncertainty in the identified parameters. Traditional deterministic methods cannot address this uncertainty. A novel approach, which integrates an advanced particle swarm optimization algorithm (APSO) and the stochastic perturbation collocation method (SPC), is proposed to address this issue, called APSO-SPC for short. The APSO algorithm improves the heterogeneous comprehensive learning particle swarm optimization algorithm (HCLPSO) based on the dynamic evolution sequence (DES), improving computational efficiency for each deterministic parameter identification process. Furthermore, the SPC method accurately estimates the means and standard deviations of uncertain parameters. Three numerical examples demonstrate the accuracy and efficiency of the APSO-SPC method in assessing parameter uncertainties caused by random measurement errors.

**Keywords:** uncertainty analysis; parameter identification; measurement errors; stochastic perturbation collocation method; heterogeneous comprehensive learning particle swarm optimization

**Mathematics Subject Classification:** 68T20, 91G60

---

**Abbreviations:** APSO-SPC: the method combining an advanced particle swarm optimization algorithm and the stochastic perturbation collocation method; SPC: stochastic perturbation collocation method;

HCLPSO: heterogeneous comprehensive learning particle swarm optimization algorithm; DES: dynamic evolution sequence; APSO: advanced particle swarm optimization algorithm; MC: Monte Carlo method; SPM: stochastic perturbation method; PSO: particle swarm optimization

## 1. Introduction

With the development of engineering technology, system parameters are difficult to calculate directly from physical equations due to factors such as structural complexity [1], material heterogeneity [2], and measurement challenges and errors [3]. To ensure the safety and reliability of engineering structures, it is often necessary to infer system parameters based on known system models and responses, known as parameter identification [4,5]. Parameter identification has been widely applied in various engineering fields, including mechanics, construction, and materials. Using an improved Kriging surrogate model and evolutionary algorithm, Han et al. [6] proposed a multipoint additional criterion and identified the parameters of nonlinear rotor-bearing system. Wang et al. [7] replaced finite element analysis with an integrated surrogate model and used the Jaya algorithm to obtain concrete thermal parameters. Roux et al. [8] identified material parameters using the efficient global optimization and the Kriging model. However, previous studies have primarily focused on the identification of deterministic parameters.

Normally, parameter identification is based on measurement data and performs parameter inversion through optimization algorithms. However, measurement errors are inevitably introduced when measuring structural responses [9]. These measurement errors tend to be random. The uncertainty in measurement data inevitably leads to uncertainty in the parameters to be identified [10]. Unlike obtaining accurate parameter values under deterministic conditions, the parameter identification problem with uncertainty caused by random measurement errors requires the assessment of the statistical characteristics of these uncertain parameters, such as means and standard deviations [11]. There is relatively little research on quantifying the uncertainty in parameter identification. Quantifying uncertainty requires a sufficient number of samples, which implies repetitive deterministic optimization processes and results in high computational costs. Therefore, there is a need for a suitable uncertainty analysis method to address such problems.

When statistically analyzing uncertain quantities, methods such as the Monte Carlo method (MC) [12,13], the stochastic perturbation method (SPM) [14–16], Bayesian inference [17], and variational inference [18] can be employed. MC is the most widely used method, suitable for the statistics of various uncertain quantities. Since the accuracy of MC in estimating uncertainties depends on the sample size, a large number of parameter identification processes are required to obtain sufficient samples, resulting in significant computational costs [19,20]. Compared with MC, SPM does not require plenty of samples to estimate results and demands fewer computational resources. However, SPM involves the calculation of derivatives of random quantities with respect to random variables, and the computational effort grows exponentially as the number of random variables increases [21]. Bayesian inference and variational inference are both highly effective methods. However, in parameter identification problem, mathematical expressions such as prior probabilities and likelihood functions are not easily formulated. Moreover, the accuracy of inference depends on the quantity of observational data. Higher accuracy leads to more deterministic parameter

identification processes, which incurs significant time costs. We need a stochastic analysis method that is computationally simple and does not require a large number of samples.

Wu et al. [22,23] proposed the stochastic perturbation collocation (SPC) method based on random perturbation theory. This method constructs the expressions for the mean and variance of random quantities by selecting specific collocation points. The computational format is simple, as it does not require the derivatives of random quantities with respect to the random variables. The number of collocation points needed is low, which means the number of repetitive deterministic sampling steps is low, making SPC well-suited for our problem. Currently, SPC has been applied in various stochastic engineering problems [24–27] but has not yet been used to assess the statistical characteristics of parameters with uncertainty to be identified. This paper is the first to consider using SPC to quantify the uncertainty of parameters, addressing the parameter identification problem with random measurement errors. Since SPC involves multiple deterministic parameter identification iterations, improving each iteration's efficiency is crucial for overall computational enhancement.

The most critical aspect is enhancing the optimization algorithm's ability to search for optimal solutions. In recent years, research on efficient intelligent optimization algorithms [28,29] has gradually matured. Among them, Lynn proposed HCLPSO [30]. This optimization algorithm has outstanding global and local search capabilities and is considered one of the excellent variants of the particle swarm optimization algorithm (PSO) [31,32]. This method has been widely applied in parameter identification. Hachana et al. [33] used root mean square error as the fitness function and identified the electrical model parameters of photovoltaic module/string with HCLPSO. Zhu et al. [34] introduced a hybrid objective function by minimizing the discrepancies between the measured and calculated natural frequencies and the correlation function vector of acceleration of damaged and intact structures and identified local damages using HCLPSO. Yousri et al. [35] analyzed the parameters of a novel fractional order dynamic photovoltaic model with HCLPSO. However, HCLPSO searches for optimal solutions by generating random point sets, which has the disadvantage of uneven distribution, making it difficult to cover the search space effectively. Overcoming this disadvantage and further enhancing the global search capability of HCLPSO would significantly improve computational efficiency.

This paper improves HCLPSO based on a low-discrepancy sequence, dynamic evolution sequence (DES) [36], forming APSO, and applies it to parameter identification. APSO addresses the issue of insufficient coverage of the search domain in the original HCLPSO, enhances the global search capability, and can significantly improve the computational efficiency of deterministic parameter identification. This paper integrates deterministic parameter identification using APSO with SPC to quantify the uncertainty of parameters, resulting in the APSO-SPC method. This method not only solves the parameter identification problem with uncertainty caused by random measurement errors but also substantially reduces the computational time cost.

The remaining work of this paper is structured as follows. The parameter identification problem with random measurement errors is briefly introduced in Section 2. Section 3 elaborates on SPC for addressing the uncertainty in parameter identification caused by random measurement errors, as well as HCLPSO improvement based on DES. Three numerical examples are presented in Section 4. The first example validates the accuracy of parameter identification using APSO and its advantages compared with HCLPSO. The second and third case examples validate the accuracy of SPC in assessing the statistical properties of uncertain parameters to be identified. The conclusion is given in Section 5.

## 2. Parameter identification problem with uncertainty caused by random measurement errors

Measurement errors stem from various factors, including measurement methods, instruments, environmental conditions, and the operational skills of the measuring personnel, among others. When measurement errors are not considered, the parameter identification problem can be transformed into an optimization problem. Typically, the objective function is defined as the least squares error between the predicted values of the mathematical model and the measured values:

$$f(\mathbf{e}) := \|\hat{\mathbf{y}}(\mathbf{e}) - \mathbf{y}\|, \quad (1)$$

where  $f$  denotes the objective function,  $\mathbf{e}$  denotes the parameters to be identified,  $\hat{\mathbf{y}}$  denotes the predicted values of the model, and  $\mathbf{y}$  denotes the measured values. When considering measurement errors, the objective function for parameter identification is given by

$$f(\mathbf{e}) := \|\hat{\mathbf{y}}(\mathbf{e}) - \mathbf{y}(\boldsymbol{\xi})\|, \quad (2)$$

where  $\boldsymbol{\xi}$  denotes the measurement errors. From Eq (2), it can be seen that due to the influence of measurement errors, the objective function for each parameter identification process may vary, leading to different identified parameters. In other words, the parameters  $\mathbf{e}$  are a function of the measurement errors  $\boldsymbol{\xi}$ :

$$\mathbf{e} = \arg \min f(\mathbf{e}) := h(\boldsymbol{\xi}), \quad (3)$$

where  $g$  is the mapping relationship between the measurement errors  $\boldsymbol{\xi}$  and the parameters  $\mathbf{e}$ .

Since the measurement errors are uncertain, the identified parameters are also uncertain, making it impossible to solve for the values using deterministic parameter identification methods. Instead, uncertainty analysis methods are needed to assess the statistical characteristics of the uncertain parameters, such as the means and standard deviations. The procedure of evaluating the means and standard deviations of random parameters will be discussed in the next section.

## 3. Method of this paper

A new APSO-SPC method is proposed in this paper, which primarily addresses the parameter identification problem with uncertainty caused by random measurement errors through SPC, and reduces the computational cost of the deterministic parameter identification process using APSO. The computational format of SPC is introduced in this section first. Then how to use APSO to approach the  $g(\boldsymbol{\xi})$  values needed in the SPC's calculation process is explained.

### 3.1. Stochastic perturbation collocation method

SPC is a modified version of SPM proposed by Wu et al. [23,37], which can obtain the means and standard deviations of random quantities with a simple computational scheme and higher accuracy. In

the parameter identification problem discussed in this paper, random quantities are parameters  $\mathbf{e} = (e_1, e_2, \dots, e_D)^T$ . Measurement errors  $\boldsymbol{\xi} = (\xi_1, \xi_2, \dots, \xi_n)^T$  are  $n$ -dimensional independent random variables, all following a distribution with a mean of zero and a symmetric probability density function, with corresponding standard deviations of  $\boldsymbol{\sigma} = (\sigma_1, \sigma_2, \dots, \sigma_n)^T$ . As noted in Section 2,

$$\mathbf{e} = \arg \min \|\hat{\mathbf{y}}(\mathbf{e}) - \mathbf{y}(\boldsymbol{\xi})\| := h(\boldsymbol{\xi}). \quad (4)$$

The formula for the means of random quantities provided by SPC is

$$E[\mathbf{e}] = \mathbf{e}_0 + \frac{1}{2} \sum_{i=1}^n \frac{\mathbf{z}_i}{\rho_{iii}} + \sum_{i=1}^n \sum_{j=i+1}^n \frac{1}{\rho_{iii} \rho_{jjj}} \left( \frac{s_{i,j}}{4} - \frac{\mathbf{z}_i + \mathbf{z}_j}{2} \right) + O(\|\boldsymbol{\sigma}\|_\infty^6), \quad (5)$$

and the formula for the covariance matrix is

$$\begin{aligned} \text{cov}(\mathbf{e}, \mathbf{e}) &= \frac{1}{4} \sum_{i=1}^n \left( \frac{\mathbf{w}_i \mathbf{w}_i^T}{\rho_{iii}} + \frac{\mathbf{z}_i \mathbf{z}_i^T}{\rho_{iii}^2} (\rho_{iii} - 1) \right) \\ &+ \frac{1}{16} \sum_{i=1}^n \sum_{j=i+1}^n \frac{1}{\rho_{iii} \rho_{jjj}} (\mathbf{o}_{i,j} \mathbf{o}_{i,j}^T + \mathbf{p}_{i,j} \mathbf{p}_{i,j}^T + \mathbf{q}_{i,j} \mathbf{q}_{i,j}^T - 4\mathbf{w}_i \mathbf{w}_i^T - 4\mathbf{w}_j \mathbf{w}_j^T) + O(\|\boldsymbol{\sigma}\|_\infty^6), \end{aligned} \quad (6)$$

where the expressions for each symbol are as follows:

$$\begin{cases} \mathbf{e}_0 = h(\boldsymbol{\theta}), \quad \boldsymbol{\theta} \text{ is a zero vector with a size of } n \times 1, \\ \mathbf{z}_i = h(\mathbf{a}_i) + h(\mathbf{a}_{-i}) - 2\mathbf{e}_0, \\ s_{i,j} = h(\mathbf{a}_{i,j}) + h(\mathbf{a}_{i,-j}) + h(\mathbf{a}_{-i,j}) + h(\mathbf{a}_{-i,-j}) - 4\mathbf{e}_0, \\ \mathbf{w}_i = h(\mathbf{a}_i) - h(\mathbf{a}_{-i}), \\ \mathbf{o}_{i,j} = h(\mathbf{a}_{i,j}) + h(\mathbf{a}_{i,-j}) - h(\mathbf{a}_{-i,j}) - h(\mathbf{a}_{-i,-j}), \\ \mathbf{p}_{i,j} = h(\mathbf{a}_{i,j}) - h(\mathbf{a}_{i,-j}) + h(\mathbf{a}_{-i,j}) - h(\mathbf{a}_{-i,-j}), \\ \mathbf{q}_{i,j} = h(\mathbf{a}_{i,j}) - h(\mathbf{a}_{i,-j}) - h(\mathbf{a}_{-i,j}) + h(\mathbf{a}_{-i,-j}), \end{cases} \quad (7)$$

$$\begin{cases} \mathbf{a}_{\pm i} = \left( 0, \dots, \pm \sqrt{\rho_{iii}} \sigma_i, \dots, 0 \right)_{i-1}, \\ \mathbf{a}_{i,\pm j} = \left( 0, \dots, \sqrt{\rho_{iii}} \sigma_i, \dots, \pm \sqrt{\rho_{jjj}} \sigma_j, \dots, 0 \right)_{i-1, j-i-1, n-j}, \quad j > i, \\ \mathbf{a}_{-i,\pm j} = \left( 0, \dots, -\sqrt{\rho_{iii}} \sigma_i, \dots, \pm \sqrt{\rho_{jjj}} \sigma_j, \dots, 0 \right)_{i-1, j-i-1, n-j}, \quad j > i, \\ \rho_{iii} = \frac{E[\xi_i^4]}{\sigma_i^4}, \quad E[\xi_i] = 0 \text{ and the probability density function of } \xi_i \text{ is symmetric.} \end{cases} \quad (8)$$

The symbols in Eq (7) lack specific physical interpretations and are introduced solely to facilitate the derivation.  $\mathbf{a}_{\pm i}, \mathbf{a}_{i,\pm j}, \mathbf{a}_{-i,\pm j}$  are the specific collocation points. By calculating  $h(\mathbf{0})$ ,  $h(\mathbf{a}_{\pm i})$ ,  $h(\mathbf{a}_{i,\pm j})$ , and  $h(\mathbf{a}_{-i,\pm j})$  and performing a specific combination, Eqs (5) and (6) are obtained. It is important to note that although SPC offers many benefits, it has certain limitations: the random variables are required to be independent and their probability density functions must be symmetric. This is the prerequisite for the validity of Eqs (5) and (6). The detailed derivation of Eqs (5) and (6) can be referenced in [38].

From Eqs (5) and (6), it is known that the SPC method listed here has an accuracy of fifth-order, which is much higher than the second-order accuracy of SPM. Moreover, SPC does not require the calculation of the derivatives of  $h(\xi)$ , only the calculation of  $h(\mathbf{0})$ ,  $h(\mathbf{a}_{\pm i})$ ,  $h(\mathbf{a}_{i,\pm j})$ , and  $h(\mathbf{a}_{-i,\pm j})$ . Since there are 1  $h(\mathbf{0})$ ,  $2 \times n$   $h(\mathbf{a}_{\pm i})$ ,  $2 \times \frac{n(n-1)}{2}$   $h(\mathbf{a}_{i,\pm j})$ , and  $2 \times \frac{n(n-1)}{2}$   $h(\mathbf{a}_{-i,\pm j})$ , a total of  $2n^2 + 1$  calculations are required. In other words, the process of using the optimization algorithm to find the parameters only requires  $2n^2 + 1$  iterations, which greatly reduces the computational cost. By the way, SPC has precisions of other orders, theoretically up to an infinite order. Higher precision can handle larger coefficients of variation. The fifth-order precision of SPC is sufficient for handling cases with a coefficient of variation within 10%. Higher precision implies more collocation points. If the coefficient of variation is not large, a third-order precision computational scheme, which only requires  $2n + 1$  calculations, is enough. It can be referenced in [37]. The computational scheme for  $h(\mathbf{0})$ ,  $h(\mathbf{a}_{\pm i})$ ,  $h(\mathbf{a}_{i,\pm j})$ , and  $h(\mathbf{a}_{-i,\pm j})$  are described in the next subsection.

### 3.2. Modified HCLPSO based on DES (APSO)

HCLPSO generally generates the initial population through random sampling. The weaker uniformity reduces the coverage of the point set in the space, leading to an incomplete search by the algorithm. This section improves HCLPSO based on DES [36], forming APSO. DES is a low discrepancy sequence with excellent uniformity, which can improve the convergence efficiency of the algorithm [39–41]. For convenience, a brief introduction to the original HCLPSO algorithm process is provided first. The entire process can be found in [30].

Define the population size in the particle swarm algorithm as  $N$ , the maximum number of iterations as  $G$ , the objective function as  $f$ , and the solution (i.e., the parameters to be identified) as  $\mathbf{e} = (e_1, e_2, \dots, e_n)^T \in R^{n \times 1}$ , where  $e_i \in [a_i, b_i]$ . Define the population as

$$\mathbf{E}_g = [\mathbf{e}_{g,1}, \mathbf{e}_{g,2}, \dots, \mathbf{e}_{g,N}], \quad (9)$$

where  $g$  represents the  $g$ -th iteration step. The initial population is represented as:

$$\mathbf{E}_0 = \mathbf{A} \otimes \mathbf{I}_N + \varepsilon_0 \circ (\mathbf{B} \otimes \mathbf{I} - \mathbf{A} \otimes \mathbf{I}), \quad (10)$$

where  $\mathbf{A} = (A_1, A_2, \dots, A_n)^T$  and  $\mathbf{B} = (B_1, B_2, \dots, B_n)^T$  define the upper and lower bounds of the solution,  $\otimes$  stands for the Kronecker product,  $\circ$  stands for the Hadamard product,  $\mathbf{I}_N$  is a vector of

size  $1 \times N$ , with each element being 1, and  $\boldsymbol{\varepsilon}_0$  is a matrix of random numbers uniformly distributed between 0 and 1, with a matrix size of  $n \times N$ .

Divide the population into the exploration and exploitation subpopulations, with sizes of  $N_1$  and  $N_2$ , respectively. The velocity update formula of the exploration subpopulation is

$$\mathbf{v}_{g+1,i} = w_g \mathbf{v}_{g,i} + k_g \boldsymbol{\varepsilon}_{g,1,i} \circ (\mathbf{p}_{g,i} - \mathbf{e}_{g,i}), \quad 1 \leq i \leq N_1, \quad (11)$$

where  $\mathbf{v}_{g,i}$  is the velocity of the  $i$ -th particle at the  $g$ -th iteration,  $w_g$  is the inertia coefficient,  $k_g$  is the self-learning factor,  $\boldsymbol{\varepsilon}_{g,1,i}$  is a vector of random numbers uniformly distributed between 0 and 1, with a vector size of  $n \times 1$ , and  $\mathbf{p}_{g,i}$  is a random comprehensive learning vector.

The velocity update formula of the exploitation subpopulation is

$$\mathbf{v}_{g+1,i} = w_g \mathbf{v}_{g,i} + c_{g,1} \boldsymbol{\varepsilon}_{g,2,i} \circ (\mathbf{p}_{g,i} - \mathbf{e}_{g,i}) + c_{g,2} \boldsymbol{\varepsilon}_{g,3,i} \circ (\mathbf{e}_{g,\text{best}} - \mathbf{e}_{g,i}), \quad N_1 < i \leq N, \quad (12)$$

where  $c_{g,1} = 2.5 - 2g/G$ ,  $c_{g,2} = 0.5 + 2g/G$ ,  $\boldsymbol{\varepsilon}_{g,2,i}$  and  $\boldsymbol{\varepsilon}_{g,3,i}$  are two vectors of random numbers uniformly distributed between 0 and 1, with sizes of  $n \times 1$ , and  $\mathbf{e}_{g,\text{best}} = \arg \min (f(\mathbf{e}_{g,i}))$ ,  $1 \leq i \leq N$ .

Next, we introduce how to modify the HCLPSO. The modification idea originates from an intuitive observation: a group of birds that search for foods in an orderly and uniform manner is more efficient than a random and disordered group. We attempted to replace the random part of the HCLPSO with the low discrepancy sequence DES, yielding very good results. The way to generate DES can be referenced in [36].

We replace the random point set  $\boldsymbol{\varepsilon}_0$  in the initial population with DES  $\mathbf{P}^{(0)}$  to ensure that the population is more evenly distributed across the entire search space at the initial stage

$$\mathbf{E}_0 = \mathbf{A} \otimes \mathbf{I}_N + \mathbf{P}^{(0)} \circ (\mathbf{B} \otimes \mathbf{I} - \mathbf{A} \otimes \mathbf{I}), \quad (13)$$

where  $\mathbf{P}^{(0)}$  is a DES with a size of  $n \times N$ .

Next, revise the velocity update formulas for the exploration and exploitation subpopulations to optimize the search direction

$$\mathbf{v}_{g+1,i} = w_g \mathbf{v}_{g,i} + k_g \mathbf{P}_i^{(1)} \circ (\mathbf{p}_{g,i} - \mathbf{e}_{g,i}), \quad 1 \leq i \leq N_1, \quad (14)$$

$$\mathbf{v}_{g+1,i} = w_g \mathbf{v}_{g,i} + c_{g,1} \mathbf{P}_i^{(2)} \circ (\mathbf{p}_{g,i} - \mathbf{e}_{g,i}) + c_{g,2} \boldsymbol{\varepsilon}_{g,3,i} \circ (\mathbf{e}_{g,\text{best}} - \mathbf{e}_{g,i}), \quad N_1 < i \leq N, \quad (15)$$

where  $\mathbf{P}^{(1)} = (\mathbf{P}_1^{(1)}, \dots, \mathbf{P}_{N_1}^{(1)})$  is a DES with a size of  $n \times N_1$ , and  $\mathbf{P}^{(2)} = (\mathbf{P}_1^{(2)}, \dots, \mathbf{P}_{N_2}^{(2)})$  is a DES with a size of  $n \times N_2$ . This is the APSO algorithm. The values of  $h(\boldsymbol{\theta})$ ,  $h(\mathbf{a}_{\pm i})$ ,  $h(\mathbf{a}_{i,\pm j})$ , and  $h(\mathbf{a}_{-i,\pm j})$  can be obtained through this method.

### 3.3. Integration of APSO and SPC

All the necessary formulas have been presented. Now, we integrate APSO and SPC and provide the pseudocode for the entire parameter identification process.  $\mathbf{A}$  and  $\mathbf{B}$  depend on the possible interval estimation of the parameters. The selection of  $N_1, N_2, G, w_g, k_g$ , and  $\mathbf{p}_{g,i}$  are not unique and can be referenced in [30]. The basic principle is that the larger the values of  $N_1, N_2$ , and  $G$ , the higher the probability of the algorithm finding the solution.

#### The pseudocode of APSO-SPC.

- 
1. Input  $n, \mathbf{A}, \mathbf{B}, N_1, N_2, G; N = N_1 + N_2$ ;
  2. Generate DES  $\mathbf{P}^{(0)}, \mathbf{P}^{(1)}$  and  $\mathbf{P}^{(2)}$ ;
  3. For every collocation point  $\mathbf{a}$  (i.e.,  $\mathbf{0}, \mathbf{a}_{\pm i}, \mathbf{a}_{i,\pm j}$  or  $\mathbf{a}_{-i,\pm j}$ );
  4. Initialize population  $\mathbf{E}_0$  according to Eq (13);
  5.  $g = 0$ ;
  6. While  $g < G$
  7.  $g = g + 1$ ;
  8. Find  $\mathbf{e}_{g,\text{best}} = \arg \min (\|\hat{\mathbf{y}}(\mathbf{e}_g) - \mathbf{y}(\mathbf{a})\|)$ ;
  9. If  $\|\hat{\mathbf{y}}(\mathbf{e}_g) - \mathbf{y}(\mathbf{a})\| < e_{\text{tol}}$ ;
  10. Break
  11. End
  12. For  $i = 1 : N$
  13. If  $1 \leq i \leq N_1$
  14. Update  $\mathbf{v}_{g+1,i}$  according to Eq (14);
  15. Else
  16. Update  $\mathbf{v}_{g+1,i}$  according to Eq (15);
  17. End
  18.  $\mathbf{e}_{g+1,i} = \mathbf{e}_{g,i} + \mathbf{v}_{g+1,i}$ ;
  19. Constrain  $\mathbf{e}$  within  $\mathbf{A}$  and  $\mathbf{B}$ ;
  20. End
  21. End
  22. Find  $\mathbf{e}_{G,\text{best}} = \arg \min (\|\hat{\mathbf{y}}(\mathbf{e}_G) - \mathbf{y}(\mathbf{a})\|)$ ;
  23. Output  $\mathbf{e}_{G,\text{best}}$  as the solution  $h(\mathbf{a})$ ;
  24. End;  $h(\mathbf{0}), h(\mathbf{a}_{\pm i}), h(\mathbf{a}_{i,\pm j})$  and  $h(\mathbf{a}_{-i,\pm j})$  are obtained now;
  25. Obtain means of uncertain parameters according to Eq (5);
  26. Obtain covariance matrix of uncertain parameters according to Eq (6).
- 

Here,  $e_{\text{tol}}$  is a small constant used to determine whether convergence has been achieved. Usually, it is not necessary to iterate  $G$  times for the algorithm to converge. At this point, the value of  $\|\hat{\mathbf{y}}(\mathbf{e}_G) - \mathbf{y}(\mathbf{a})\|$  is very close to zero. If convergence fails, try using larger  $N$  and  $G$ .



## 4. Numerical examples

### 4.1. Cantilever beam

Beams are one of the most common structures and have significant practical relevance. Due to their simple structure and the availability of extensive research results, beams are well-suited as numerical examples to validate the effectiveness of our algorithm.

#### 4.1.1. Parameter identification based on APSO

To validate the superiority of APSO in parameter identification over HCLPSO, this example considers the parameter identification of a cantilever beam fixed at one end and free at the other. The length of the cantilever beam,  $L = 3\text{m}$ , is subjected to a downward concentrated force  $F = F_0(1 + e_1)$  at  $a = a_0(1 + e_2)$ , where  $a_0 = 0.8L$ ,  $F_0 = 5 \times 10^5 \text{N}$ , and the possible range for  $e_1$  and  $e_2$  is both  $[-0.2, 0.2]$ .  $F$  and  $a$  are the parameters to be identified. According to the mechanics of materials, the deflection at any position  $x$  on the cantilever beam can be expressed as

$$u = \begin{cases} \frac{-Fx^2}{6EI}(3a - x), & 0 \leq x \leq a \\ \frac{-Fa^2}{6EI}(3x - a), & a \leq x \leq L \end{cases},$$

where  $I = 0.0000833\text{m}^4$  is the moment of inertia, and  $E = 2 \times 10^{11} \text{Pa}$  is the elastic modulus.

To identify the parameters  $F$  and  $a$ , measurement points are set on the cantilever beam to measure the deflection values. In this subsection, two measurement points are set at  $x_1 = 0.6L$  and  $x_2 = 0.4L$  on the cantilever beam. The measured deflection values at these points are  $u_1 = -0.087\text{m}$  and  $u_2 = -0.043\text{m}$ , respectively. By substituting  $u_1$  and  $u_2$  into the deflection expression, the true parameters can be calculated as  $F = 5 \times 10^5 \text{N}$  and  $a = 2.4\text{m}$ . The least squares error between the predicted deflection values and the actual deflection values at the two measurement points is used as the objective function. Both APSO and HCLPSO are employed for optimization and eventually converge to the true values, indicating that both APSO and HCLPSO have good parameter identification accuracy.

**Table 1.** Comparison of the convergence steps of HCLPSO and APSO.

Variable name	$F$ (N)			$a$ (m)		
Relative error	1%	0.1%	0.01%	1%	0.1%	0.01%
HCLPSO	51	223	402	41	227	385
APSO	46	146	270	23	130	243

To further compare the computational performance of the two algorithms, they were run 30 times each, and the average number of convergence steps when the relative error of the parameters with the true values was 1%, 0.1%, and 0.01% are statistically analyzed. The results are listed in Table 1. Under

different error standards, the percentage increase in speed is used as a measure of speed improvement. To quantitatively measure the degree of speed improvement, the relative speedup is introduced:

$$\text{Relative speedup} = \frac{|\text{HCLPSO convergence steps} - \text{DES-PSO convergence steps}|}{\text{DES-PSO convergence steps}} \times 100\% .$$

From Table 1, when the relative error converges to 1%, APSO identifies the parameters  $F$  and  $a$  with relative speedups of 10.87% and 78.26%, respectively. When converging to 0.1%, APSO has relative speedups of 52.74% and 74.62%. When converging to 0.01%, APSO has relative speedups of 48.89% and 58.44%. In summary, APSO is more computationally efficient in parameter identification.

#### 4.1.2. Parameter identification with random measurement errors

During the measurement of measurement points, measurement errors often occur, leading to discrepancies between actual measured values and true values [42]. In this example, it is assumed that the deflection values  $u_1$  and  $u_2$  measured in Section 4.1.1 have the same measurement error  $v$ , which is uniformly distributed over  $[-0.001\text{m}, 0.001\text{m}]$ . Due to errors in the measured deflection values  $u_1$  and  $u_2$ , the calculated concentrated force  $F$  and the position  $a$  will also deviate from the true values. Although the true values cannot be precisely determined, statistical data of the parameters can be analyzed.

SPC is employed to obtain the means and standard deviations of the parameters. MC is performed with 100000 samples, whose results are considered reference solutions to test the accuracy of SPC.

The means and standard deviations of the concentrated force  $F$  and the position  $a$  computed by MC and SPC are shown in Table 2. It can be observed from Table 2 that: the means calculated by SPC are within 0.06% of those calculated by MC; the standard deviations calculated by SPC have an error within 2.78% of those calculated by MC. This indicates that SPC can achieve high accuracy with limited computational cost.

**Table 2.** Comparison of results between MC and SPC.

	MC(100,000 times)	SPC	relative error
Mean of $F$ (N)	499824.13	500003.66	0.04%
Standard deviation of $F$ (N)	73175.83	73131.47	0.06%
Mean of $a$ (m)	2.4418	2.4403	0.06%
Standard deviation of $a$ (m)	0.2854	0.2775	2.78%

Additionally, Table 2 indicates that although the measurement error is minimal, it can still result in coefficients of variation of 14.63% for parameter  $F$  and 11.37% for parameter  $a$ . Even minor variations can significantly impact the outcomes of engineering analyses, which underscores the importance of analyzing the uncertainty in parameter identification caused by random measurement errors.

#### 4.2. Parameter identification of cement with random measurement errors in extremely cold regions

Building structures in extremely cold regions are often subject to cracking due to low temperatures [43–45]. To ensure the reliability of these structures, it is necessary to have an appropriate filler ratio and good curing methods, as well as cement materials suitable for cold regions. This example considers a batch of molded cement and analyzes its construction conditions. Ref. [46] provides a mathematical model of the performance of cement and related influencing factors, as seen in Table 3. By measuring the strength  $y_1$ , slump  $y_2$ , and cement consumption  $y_3$ , and using the least squares error between predicted and measured values as the objective function, HCLPSO and APSO are both employed for optimization to analyze the environmental temperature  $e_1$ , the cement-sand mass ratio  $e_2$  and the solid phase mass fraction of the slurry  $e_3$  during the construction of this batch of cement. There is a certain degree of error associated with the measurements, and it is assumed that the measurement errors follow a uniform distribution. The distribution range of the measured variables and the parameters to be identified can be found in Table 4.

**Table 3.** Mathematical model of measured variables and parameters to be identified.

Measured variables	Mathematical model
Strength $y_1$ (MPa)	$y_1 = 41.189410 + 0.022597e_1 - 121.121930e_2 - 1.030760e_3 + 1.454270e_2e_3 + 119.68705e_2^2 + 6.456120 \times 10^{-3}e_3^2$
Slump $y_2$ (cm)	$y_2 = 68.045440 - 0.046469e_1 - 4.05172e_2 - 0.609680e_3$
Cement consumption $y_3$ ( $\text{kg} \cdot \text{m}^{-3}$ )	$y_3 = -583.53735 + 1080.22956e_2 + 8.27441e_3$

**Table 4.** Distribution intervals for the measured variables and parameters to be identified.

Measured variables	Distribution interval	Parameters to be identified	Possible distribution interval
Strength $y_1$ (MPa)	[0.535, 0.545]	Curing temperature $e_1$ ( $^{\circ}\text{C}$ )	[0, 25]
Slump $y_2$ (cm)	[27.5, 28.5]	Cement-to-sand ratio $e_2$ (1)	[0.1, 0.2]
Cement consumption $y_3$ ( $\text{kg} \cdot \text{m}^{-3}$ )	[95, 105]	Solid phase mass fraction of slurry $e_3$ (%)	[60, 80]

We first examine the convergence behavior of the optimization algorithm.  $G$  is chosen as 300 and different values of  $N_1$  and  $N_2$  are chosen to compare the convergence behavior.

From Figure 1, we can observe that as the number of particles increases and the number of iterations grows, it becomes easier for the algorithm to find the optimal solution. Despite the randomness, APSO converges faster than HCLPSO in most cases. If the number of particles is insufficient, the algorithm cannot converge effectively. On the other hand, too many particles do not significantly improve the convergence speed and lead to waste. An appropriate number of particles ensures a good convergence speed without excessive time cost. We adopt  $N_1 = 30$  and  $N_2 = 50$  for the subsequent calculations.

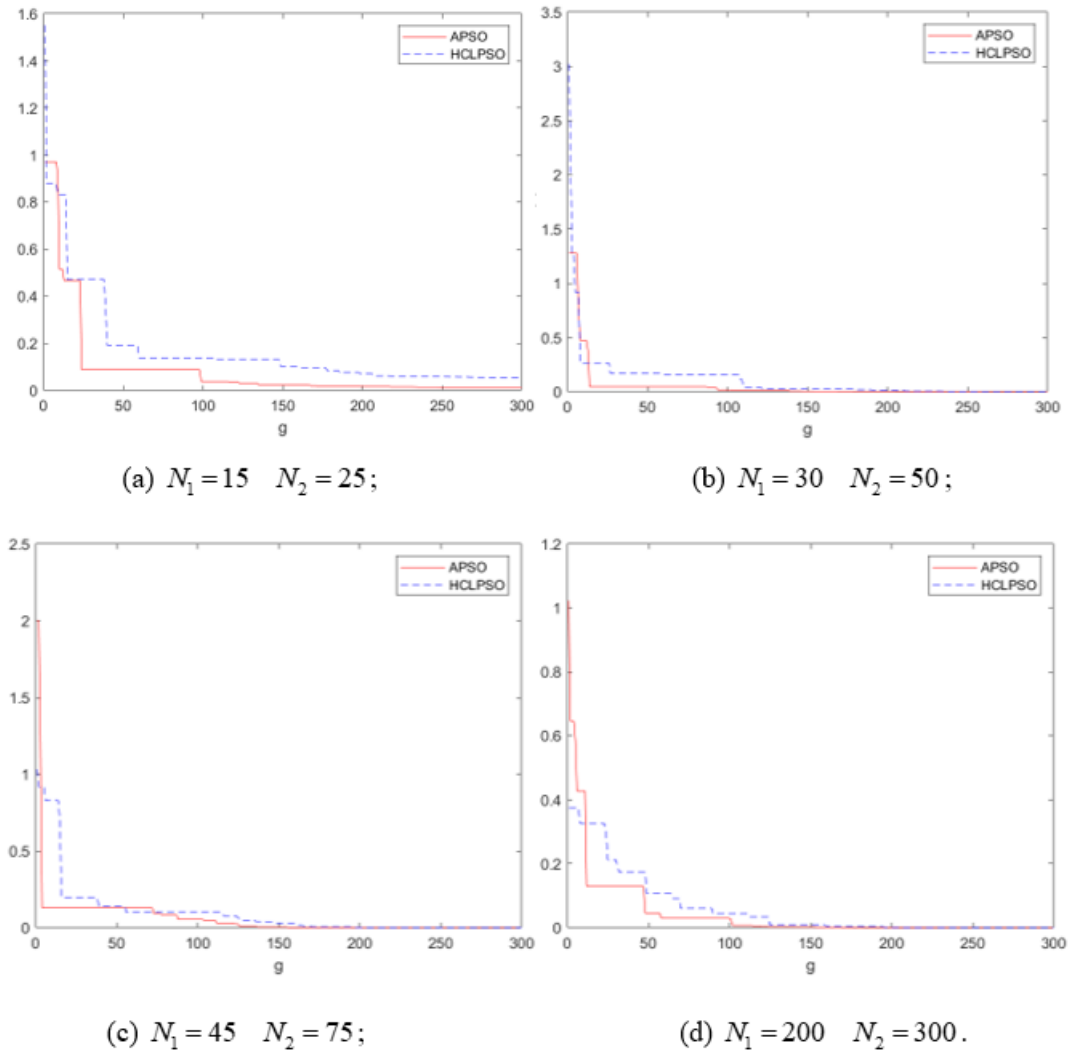


**Figure 1.** The convergence of the objective function  $f(e)$ .

In this problem, the number of random errors is  $n = 3$ , which means  $2n^2 + 1 = 19$  deterministic optimization processes are required. For a personal computer, APSO takes approximately 0.1013 seconds to complete one deterministic optimization process, while HCLPSO takes about 0.1417 seconds. The total time for APSO-SPC is approximately 1.9547 seconds, while the total time for HCLPSO+SPC is approximately 2.7134 seconds. It is obvious that computing the derivatives of the random quantities  $e_1$ ,  $e_2$ , and  $e_3$  with respect to random measurement errors are not realistic, and thus SPM cannot be used. If we use MC, the number of deterministic optimization processes required will be significantly large, 100,000 MC simulations would take approximately 10,130 seconds. It can be concluded that SPC exhibits a distinct advantage concerning computational efficiency. The next step is to assess its accuracy. The SPC and MC are used to calculate the means and standard deviations of the parameters, with the MC results serving as the benchmark for evaluation. The results can be seen in Table 5.

**Table 5.** Comparison of results between SPC and MC.

	MC (100,000 runs)	SPC	Relative error
Mean of $e_1$ (°C)	17.90954766	18.10020748	1.06%
Standard deviation of $e_1$ (°C)	1.140044345	1.123606971	1.44%
Mean of $e_2$ (1)	0.147621727	0.147735203	0.08%
Standard deviation of $e_2$ (1)	0.004125800	0.004061462	1.56%
Mean of $e_3$ (%)	63.33780769	63.32166274	0.03%
Standard deviation of $e_3$ (%)	0.435925564	0.429374577	1.50%

The results indicate that the relative error of the means obtained by SPC and MC with 100,000 runs is within 1.06%, and the relative error of the standard deviations is within 1.56%. Therefore, this numerical example proves that APSO-SPC has good accuracy and applicability in the cement construction information identification problem with uncertainty caused by random measurement errors.

## 5. Conclusions

To solve the parameter identification problem with uncertainty caused by random measurement errors, a new APSO-SPC method is proposed in this paper. Utilizing SPC for uncertainty analysis allows for the assessment of the statistical characteristics of the parameters with uncertainty, effectively tackling the issue of uncertain parameter identification. Additionally, the incorporation of the APSO enhances the search domain coverage that was previously inadequate in HCLPSO, thereby improving computational efficiency for each parameter identification instance and substantially reducing the computational time costs. Through three distinct numerical examples, this paper validates the accuracy of APSO in parameter identification and its greater computational efficiency compared with HCLPSO, and the accuracy of SPC in quantifying the statistical information of parameter identification uncertainty caused by stochastic measurement errors is validated.

The novel approach we propose, Optimization Algorithm integrated with SPC, can address the parameter identification problem with uncertainty caused by random measurement errors. The APSO we developed is not the only option. Any advanced optimization algorithm can be tried. Adopting emerging technologies can lead to optimistic outcomes.

The approach outlined in this paper is utilized for static parameter identification. Future endeavors will consider extending the application of this precise and efficient method to the dynamic parameter identification problem present in nonlinear dynamical systems [47–50]. The issues that need to be addressed include the proper modeling of the dynamic system, and modeling the mathematical relationship between the measured variables and the system parameters.

## Author contributions

Peng Zhong: Methodology, investigation, software, validation, writing—original draft, writing—review and editing; Xuanlong Wu: Methodology, software, project administration, supervision,

funding acquisition, writing–review and editing; Li Zhu: Methodology, writing–review & editing, investigation; Aohao Yang: Methodology. investigation. All authors have read and approved the final version of the manuscript for publication.

### Use of AI tools declaration

The authors declare they have not used Artificial Intelligence (AI) tools in the creation of this article.

### Acknowledgments

This work was supported by the National Natural Science Foundation of China (Nos. 12372190 and 62388101).

### Conflict of interest

The authors declare that they have no competing interests.

### References

1. W. C. Xing, Y. Q. Wang, A unified nonlinear dynamic model for bolted flange joint disk-drum structures under different interface states: theory and experiment, *Appl. Math. Model.*, **137** (2025), 115695. <https://doi.org/10.1016/j.apm.2024.115695>
2. D. W. Huang, Y. L. Zhao, K. Q. Ye, F. Wu, H. W. Zhang, W. X. Zhong, The efficient calculation methods for stochastic nonlinear transient heat conduction problems, *J. Comput. Sci.*, **67** (2023), 101939. <https://doi.org/10.1016/j.jocs.2022.101939>
3. Y. R. Hong, Nonlinear modeling of measurement errors in gateway energy meters, *Measurement: Sensors*, **35** (2024), 101286. <https://doi.org/10.1016/j.measen.2024.101286>
4. F. Wu, L. Zhu, Y. L. Zhao, C. F. Ai, X. Wang, F. Cai, et al., Wave spectrum fitting with multiple parameters based on optimization algorithms and its application, *Ocean Eng.*, **312** (2024), 119073. <https://doi.org/10.1016/j.oceaneng.2024.119073>
5. H. Y. Zeng, Z. F. Lin, G. H. Huang, X. Q. Yang, Y. F. Li, J. B. Su, et al., Parameter identification of DEM-FEM coupling model to simulate traction behavior of tire-soil interaction, *J. Terramechanics*, **117** (2025), 101012. <https://doi.org/10.1016/j.jterra.2024.101012>
6. F. Han, X. L. Guo, C. Mo, H. Y. Gao, P. J. Hou, Parameter identification of nonlinear rotor-bearing system based on improved kriging surrogate model, *J. Vib. Control*, **23** (2017), 794–807. <https://doi.org/10.1177/1077546315585242>
7. F. Wang, C. J. Zhao, Y. H. Zhou, H. W. Zhou, Z. P. Liang, F. Wang, et al., Multiple thermal parameter inversion for concrete dams using an integrated surrogate model, *Appl. Sci.*, **13** (2023), 5407. <https://doi.org/10.3390/app13095407>

8. E. Roux, Y. Tillier, S. Kraria, P. Bouchard, An efficient parallel global optimization strategy based on Kriging properties suitable for material parameters identification, *Arch. Mech. Eng.*, **67** (2020), 131689. <https://doi.org/10.24425/ame.2020.131689>
9. C. Ding, S. X. Pei, H. Q. Chen, Y. Huang, B. Meng, L. Liu, Effect of clearance on measuring accuracy in two-dimensional piston flowmeter, *Flow Meas. Instrum.*, **99** (2024), 102673. <https://doi.org/10.1016/j.flowmeasinst.2024.102673>
10. S. Dorvash, S. N. Pakzad, Effects of measurement noise on modal parameter identification, *Smart Mater. Struct.*, **21** (2012), 065008. <https://doi.org/10.1088/0964-1726/21/6/065008>
11. F. Wu, W. X. Zhong, A hybrid approach for the time domain analysis of linear stochastic structures, *Comput. Method. Appl. M.*, **265** (2013), 71–82. <https://doi.org/10.1016/j.cma.2013.06.006>
12. D. W. Huang, F. Wu, Y. L. Zhao, J. Yan, H. W. Zhang, Application of high-credible statistical results calculation scheme based on least squares Quasi-Monte Carlo method in multimodal stochastic problems, *Comput. Method. Appl. M.*, **418** (2024), 116576. <https://doi.org/10.1016/j.cma.2023.116576>
13. H. T. Podeh, A. Parsaie, B. Shahinejad, A. Arshia, Z. Shamsi, Development and uncertainty analysis of infiltration models using PSO and Monte Carlo method, *Irrig. Drain.*, **72** (2023), 38–47. <https://doi.org/10.1002/ird.2769>
14. F. Wu, D. W. Huang, X. M. Xu, K. Zhao, N. Zhou, An adaptive divided-difference perturbation method for solving stochastic problems, *Struct. Saf.*, **103** (2023), 102346. <https://doi.org/10.1016/j.strusafe.2023.102346>
15. M. Kamiński, Uncertainty analysis in solid mechanics with uniform and triangular distributions using stochastic perturbation-based Finite Element Method, *Finite Elem. Anal. Des.*, **200** (2022), 103648. <https://doi.org/10.1016/j.finel.2021.103648>
16. L. Zhu, K. Q. Ye, D. W. Huang, F. Wu, W. X. Zhong, An adaptively filtered precise integration method considering perturbation for stochastic dynamics problems, *Acta Mech. Solida Sin.*, **36** (2023), 317–326. <https://doi.org/10.1007/s10338-023-00381-4>
17. A. Pavone, A. Merlo, S. Kwak, J. Svensson, Machine learning and Bayesian inference in nuclear fusion research: an overview, *Plasma Phys. Control. Fusion*, **65** (2023), 053001. <https://doi.org/10.1088/1361-6587/acc60f>
18. M. Welandawe, M. R. Andersen, A. Vehtari, J. H. Huggins, A framework for improving the reliability of black-box variational inference, *J. Mach. Learn. Res.*, **25** (2024), 1–71.
19. J. C. Rodrigues, J. Facão, M. J. Carvalho, Parameter identification and uncertainty evaluation in Quasi-Dynamic test of solar thermal collectors with Monte Carlo method, *Renew. Energ.*, **236** (2024), 121403. <https://doi.org/10.1016/j.renene.2024.121403>
20. P. Z. Pan, F. S. Su, H. J. Chen, S. L. Yan, X. T. Feng, F. Yan, Uncertainty analysis of rock failure behaviour using an integration of the probabilistic collocation method and elasto-plastic cellular automaton, *Acta Mech. Solida Sin.*, **28** (2015), 536–555. [https://doi.org/10.1016/S0894-9166\(15\)30048-3](https://doi.org/10.1016/S0894-9166(15)30048-3)
21. M. Y. Feng, T. J. Sun, Adaptive perturbation method for optimal control problem governed by stochastic elliptic PDEs, *Comp. Appl. Math.*, **43** (2024), 100. <https://doi.org/10.1007/s40314-024-02607-8>

22. F. Wu, K. Zhao, L. L. Zhao, C. Y. Chen, W. X. Zhong, Uncertainty analysis of the control rod drop based on the adaptive collocation stochastic perturbation method, *Ann. Nucl. Energy*, **190** (2023), 109873. <https://doi.org/10.1016/j.anucene.2023.109873>
23. F. Wu, Q. Gao, X. M. Xu, W. X. Zhong, A modified computational scheme for the stochastic perturbation finite element method, *Lat. Am. J. Solids Struct.*, **12** (2015), 2480–2505. <https://doi.org/10.1590/1679-78251772>
24. Z. J. Shao, X. M. Li, P. Xiang, A new computational scheme for structural static stochastic analysis based on Karhunen-Loève expansion and modified perturbation stochastic finite element method, *Comput. Mech.*, **71** (2023), 917–933. <https://doi.org/10.1007/s00466-022-02259-7>
25. S. Chakraborty, S. Adhikari, R. Ganguli, The role of surrogate models in the development of digital twins of dynamic systems, *Appl. Math. Model.*, **90** (2021), 662–681. <https://doi.org/10.1016/j.apm.2020.09.037>
26. Z. J. Shao, Q. Xia, P. Xiang, H. Zhao, L. Z. Jiang, Stochastic free vibration analysis of FG-CNTRC plates based on a new stochastic computational scheme, *Appl. Math. Model.*, **127** (2024), 119–142. <https://doi.org/10.1016/j.apm.2023.11.016>
27. S. Z. Feng, Q. J. Sun, S. Xiao, X. Han, Y. B. Li, Z. X. Li, A novel multi-physics coupling model for the stochastic analysis of phased arrays considering material spatial uncertainty, *Appl. Math. Model.*, **128** (2024), 707–722. <https://doi.org/10.1016/j.apm.2024.01.042>
28. Y. X. Yang, K. Zhao, Y. L. Zhao, F. Wu, C. Y. Chen, J. Yan, et al., UA-CRD, a computational framework for uncertainty analysis of control rod drop with time-variant epistemic uncertain parameters, *Ann. Nucl. Energy*, **195** (2024), 110171. <https://doi.org/10.1016/j.anucene.2023.110171>
29. F. Wu, Y. L. Zhao, Y. X. Yang, X. P. Zhang, N. Zhou, A new discrepancy for sample generation in stochastic response analyses of aerospace problems with uncertain parameter, *Chinese J. Aeronaut.*, **37** (2024), 192–211. <https://doi.org/10.1016/j.cja.2024.09.044>
30. N. Lynn, P. N. Suganthan, Heterogeneous comprehensive learning particle swarm optimization with enhanced exploration and exploitation, *Swarm Evol. Comput.*, **24** (2015), 11–24. <https://doi.org/10.1016/j.swevo.2015.05.002>
31. E. Zhang, Z. H. Nie, Q. Yang, Y. Q. Wang, D. Liu, S. Jeon, et al., Heterogeneous cognitive learning particle swarm optimization for large-scale optimization problems, *Inform. Sciences*, **633** (2023), 321–342. <https://doi.org/10.1016/j.ins.2023.03.086>
32. T. Jeyaraman, D. Joelpraveenkumar, M. Kaliraj, M. K. Chandar, M. W. Iruthayarajan, Tuning of MIMO PID controller using HCLPSO algorithm, In: *Proceedings of international conference on power electronics and renewable energy systems*, Singapore: Springer, 2022, 377–385. [https://doi.org/10.1007/978-981-16-4943-1\\_35](https://doi.org/10.1007/978-981-16-4943-1_35)
33. O. Hachana, B. Aoufi, G. M. Tina, M. A. Sid, Photovoltaic mono and bifacial module/string electrical model parameters identification and validation based on a new differential evolution bee colony optimizer, *Energ. Convers. Manage.*, **248** (2021), 114667. <https://doi.org/10.1016/j.enconman.2021.114667>
34. J. J. Zhu, M. Huang, Z. R. Lu, Bird mating optimizer for structural damage detection using a hybrid objective function, *Swarm Evol. Comput.*, **35** (2017), 41–52. <https://doi.org/10.1016/j.swevo.2017.02.006>



35. D. Yousri, D. Allam, M. B. Eteiba, P. N. Suganthan, Static and dynamic photovoltaic models' parameters identification using chaotic heterogeneous comprehensive learning particle swarm optimizer variants, *Energ. Convers. Manage.*, **182** (2019), 546–563. <https://doi.org/10.1016/j.enconman.2018.12.022>
36. F. Wu, Y. L. Zhao, K. Zhao, W. X. Zhong, A multi-body dynamical evolution model for generating the point set with best uniformity, *Swarm Evol. Comput.*, **73** (2022), 101121. <https://doi.org/10.1016/j.swevo.2022.101121>
37. F. Wu, W. X. Zhong, A modified stochastic perturbation method for stochastic hyperbolic heat conduction problems, *Comput. Method. Appl. M.*, **305** (2016), 739–758. <https://doi.org/10.1016/j.cma.2016.03.032>
38. K. Zhao, X. M. Xu, C. Y. Chen, F. Wu, D. W. Huang, Y. Y. Xi, et al., Nonlinear state equation and adaptive symplectic algorithm for the control rod drop, *Ann. Nucl. Energy*, **179** (2022), 109402. <https://doi.org/10.1016/j.anucene.2022.109402>
39. J. Kudela, R. Matousek, Recent advances and applications of surrogate models for finite element method computations: a review, *Soft Comput.*, **26** (2022), 13709–13733. <https://doi.org/10.1007/s00500-022-07362-8>
40. F. Wu, Y. L. Zhao, J. H. Pang, J. Yan, W. X. Zhong, Low-discrepancy sampling in the expanded dimensional space: an acceleration technique for particle swarm optimization, 2023, arXiv:2303.03055.
41. Y. L. Zhao, F. Wu, J. H. Pang, W. X. Zhong, Updating velocities in heterogeneous comprehensive learning particle swarm optimization with low-discrepancy sequences, 2022, arXiv:2209.09438.
42. Q. X. Zhuang, N. Wan, Y. H. Guo, Z. Y. Chang, Z. Wang, Uncertainty propagation and assessment of five-axis on-machine measurement error, *J. Manuf. Sci. Eng.*, **144** (2022), 101004. <https://doi.org/10.1115/1.4054286>
43. C. C. Wen, P. Zhang, J. Wang, S. W. Hu, Influence of fibers on the mechanical properties and durability of ultra-high-performance concrete: a review, *J. Build. Eng.*, **52** (2022), 104370. <https://doi.org/10.1016/j.jobbe.2022.104370>
44. N. Ankur, N. Singh, Performance of cement mortars and concretes containing coal bottom ash: a comprehensive review, *Renew. Sust. Energ. Rev.*, **149** (2021), 111361. <https://doi.org/10.1016/j.rser.2021.111361>
45. H. Huang, Y. J. Yuan, W. Zhang, L. Zhu, Property assessment of high-performance concrete containing three types of fibers, *Int. J. Concr. Struct. Mater.*, **15** (2021), 39. <https://doi.org/10.1186/s40069-021-00476-7>
46. G. Y. Zhao, J. Ma, K. Peng, Q. Yang, L. Zhou, Mix ratio optimization of alpine mine backfill based on the response surface method, *Chinese Journal of Engineering*, **35** (2013), 559–565. <https://doi.org/10.13374/j.issn1001-053x.2013.05.003>
47. F. Wu, K. Zhao, X. L. Wu, H. J. Peng, L. L. Zhao, W. X. Zhong, A time-averaged method to analyze slender rods moving in tubes, *Int. J. Mech. Sci.*, **279** (2024), 109510. <https://doi.org/10.1016/j.ijmecsci.2024.109510>
48. F. M. A. AL-Gaadi, F. Alemdar, Dynamic parameter identification of cold-formed storage rack systems using shaking table test, *Results in Engineering*, **22** (2024), 102160. <https://doi.org/10.1016/j.rineng.2024.102160>

49. F. Wu, W. X. Zhong, Constrained Hamilton variational principle for shallow water problems and Zu-class symplectic algorithm, *Appl. Math. Mech.*, **37** (2016), 1–14.  
<https://doi.org/10.1007/s10483-016-2051-9>
50. Q. Gao, F. Wu, H. W. Zhang, W. X. Zhong, W. P. Howson, F. W. Williams, A fast precise integration method for structural dynamics problems, *Struct. Eng. Mech.*, **43** (2012), 1–13.  
<https://doi.org/10.12989/sem.2012.43.1.001>



AIMS Press

© 2025 the Author(s), licensee AIMS Press. This is an open access article distributed under the terms of the Creative Commons Attribution License (<http://creativecommons.org/licenses/by/4.0>)